

## Hyperfine-field studies of $\text{Fe}_3\text{Al}$ and $\text{Fe}_{3-x}\text{Cr}_x\text{Al}$ alloys

N. Lakshmi, K. Venugopalan, and J. Varma

*Physics Department, M. L. Sukhadia University, Udaipur 313 001, India*

(Received 12 August 1992)

Measurements of hyperfine fields have been performed on ordered and disordered  $\text{Fe}_3\text{Al}$  alloys and disordered  $\text{Fe}_{3-x}\text{Cr}_x\text{Al}$  alloys for  $0 \leq x \leq 1$  with use of a  $^{57}\text{Fe}$  Mössbauer technique. The Curie temperatures of all the samples were measured with use of the zero-velocity thermal-scan method. The Curie temperature decreases linearly with increasing chromium concentration. Mössbauer spectra of the samples show the presence of a paramagnetic peak coexisting with the hyperfine structure for  $x \geq 0.5$ . The spectra fitted with a hyperfine-field distribution show the presence of two hyperfine-field components. The lower of these in disordered  $\text{Fe}_3\text{Al}$  is assigned to have 5 nearest-neighbor Al atoms and the higher-field one to have 2–3 nearest-neighbor Al atoms. A systematic replacement of Fe with Cr shows a linear decrease with increasing Cr concentration for both field components. The change in the lower field is only 65 kOe while that in the higher one is 120 kOe over the entire Cr-concentration range. The rapid decrease in the high-field component with increasing Cr concentration points to the fact that despite the considerable disorder which exists, Cr preferentially substitutes for iron at sites having 2–3 nearest-neighbor Al atoms.

### I. INTRODUCTION

Extensive theoretical as well as experimental studies have been done in recent years to understand magnetic and chemical interactions in solid solutions.<sup>1–3</sup> These studies have attempted to establish correlations between different types of interactions. Many of them also examine the way and extent to which these interactions influence phase diagrams in transition-metal alloys. This becomes important because although the interaction energies are small, as compared to the alloy formation energy, they play a crucial role in determining the ground state of these systems. Here, therefore, a good understanding of environmental effects is essential.

In particular, in magnetic systems, parameters like the magnetic moment, Curie temperature, etc., are good indicators of environmental effects. A study entailing the measurement of these quantities can be made in two different ways to understand such effects in an alloy. One way is to examine any change in these quantities for a particular concentration of the alloy at various stages of long- and short-range ordering. Another approach to see environmental effects is to examine the parameters of interest as a function of the alloy composition or concentration at any particular state of ordering. Stoichiometric compositions, in particular, offer the best conditions for the latter type of studies. The chemical environment of constituents in a stoichiometric alloy which exists in the fully ordered state is well defined. This, therefore, facilitates the interpretation of measured magnetic properties in terms of the known chemical environment. However, in disordered systems, chemical ordering is limited to only the short-range type. Hence careful studies making use of a variation in stoichiometry are desirable as environmental effects are more dominant in such systems.

Magnetic properties of iron-based transition-metal alloys display a rather great sensitivity to environmental

effects. Transition-metal alloys based on Co or Ni which, like iron, are also both transitional as well as ferromagnetic, do not, however, show the same amount of sensitivity as compared to Fe-based alloys.<sup>4</sup> In iron-based transition-metal alloys of say, the  $A_3B$  type ( $\text{Fe}_3\text{Al}$  and  $\text{Fe}_3\text{Si}$  are good examples) where long-range ordering is possible, both magnetization measurements as well as microscopic measurements through NMR, Mössbauer effect, neutron scattering, etc., together allow the unambiguous assignment of distinct moment values to iron atoms. In a perfectly long-range-ordered substance where the sense of magnetization between sublattices is the same, the microscopic and macroscopic measurements usually agree.<sup>5</sup> But in the limit of short-range ordering, the microscopic and macroscopically measured quantities like the Curie temperature, average magnetic moments, etc., might show considerable differences. The Fe-Cr system is a good example of such differences.<sup>6</sup> As iron-based transition-metal alloys show a large sensitivity to the environment, an excellent method to probe microscopic properties is to use the  $^{57}\text{Fe}$  Mössbauer technique.

$\text{Fe}_3\text{Al}$  and  $\text{Fe}_3\text{Si}$  are good and well-studied examples of single-magnetic-component systems that can be studied over a wide range of composition. In the perfectly ordered state,  $\text{Fe}_3\text{Al}$  has typically the  $D0_3$  type of structure. Figure 1 shows a unit cell of  $\text{Fe}_3\text{Al}$  ordered in this structure. It consists of four face-centered-cubic sublattices  $A$ ,  $B$ ,  $C$ , and  $D$ . The iron atom occupies  $A$ ,  $B$ , and  $C$  sublattices while  $D$  is occupied by Al. Iron atom at the  $A$  sublattice is denoted by  $\text{Fe}[A]$  and is equivalent to that at the site  $C$ ,  $\text{Fe}[C]$ .  $\text{Fe}[A, C]$  therefore has four Fe and four Al as the first-nearest neighbor.  $\text{Fe}[B]$ , on the other hand, has eight Fe as first-nearest neighbor. In  $\text{Fe}_3\text{Si}$ , which is isostructural to  $\text{Fe}_3\text{Al}$ , it has been shown by Mössbauer, spin-echo, and NMR as well as neutron-diffraction techniques<sup>7–10</sup> that dilute transition-metal impurities in  $\text{Fe}_3\text{Si}$  preferentially enter one or the other of

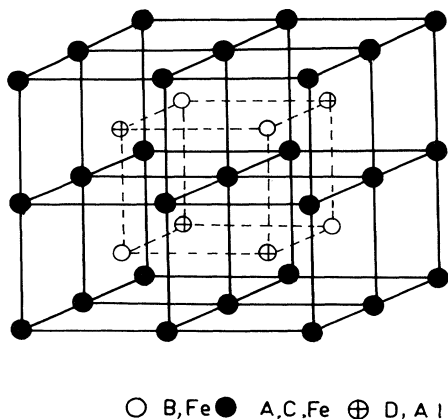


FIG. 1. Unit cell of the ordered  $\text{Fe}_3\text{Al}$  structure.

the two inequivalent iron sites. It has been found that the  $3d$  transition elements which are less electronegative than Fe (e.g., Co) preferentially occupy the  $[A, C]$  site, whereas elements which are more electronegative than Fe (e.g., Mn, V) in the periodic table preferentially occupy the  $[B]$  site. In  $\text{Fe}_3\text{Al}$ , however, no such systematic site-preference studies have been made. The type of ordering to be seen in  $\text{Fe}_3\text{Al}$  is highly sensitive to the type of heat treatment it has had<sup>11</sup> and can be held at almost any degree of ordering to be studied. In the present investigation, our aim has been to study the effect of replacement of Fe with Cr progressively, starting from  $\text{Fe}_3\text{Al}$  to form the series  $\text{Fe}_{3-x}\text{Cr}_x\text{Al}$  for various Cr concentrations in disordered alloys.

## II. EXPERIMENTAL

The starting materials iron, aluminum, and chromium used for the preparation of the alloys  $\text{Fe}_3\text{Al}$  as well as the series  $\text{Fe}_{3-x}\text{Cr}_x\text{Al}$ , for  $x=0.05, 0.1, 0.5, 0.8, 0.9, 0.95$ , and  $1.0$ , were of at least 99.99% purity obtained from M/s. Spex Industries, Inc., U.S.A. These were weighed out in the desired atomic ratio and melted together in an arc furnace in argon atmosphere. The melting was carried out five times in order to homogenize the alloys. The weight loss during melting was less than 1%. The ingots obtained were crushed and ground to powder. They were then sealed into quartz ampoules evacuated to  $10^{-5}$  Torr and heated at  $800^\circ\text{C}$  for 72 h. Part of the  $\text{Fe}_3\text{Al}$  sample (sample I) as well as the  $\text{Fe}_{3-x}\text{Cr}_x\text{Al}$  were quenched to room temperature. Another part of  $\text{Fe}_3\text{Al}$  (sample II) was cooled down to room temperature at a rate of  $50^\circ\text{C}/\text{h}$ .

Samples for Mössbauer-effect studies were made to have a thickness of  $10 \text{ mg}/\text{cm}^2$  of natural iron. The required quantity of the powdered sample was weighed out and mixed thoroughly with boron nitride. They were then packed into copper rings about 1-mm thick with an effective sample area of  $1 \text{ cm}^2$ . They were then covered with Al foils. A standard Austin drive and controller assembly were used in the flyback mode. The source used was 25-mCi  $^{57}\text{Co}$  in rhodium matrix. The data were accumulated in a 512-channel multichannel analyzer

(MCA) for approximately 3 days to obtain transmission Mössbauer data of fairly good statistics. The velocity was calibrated using a laser velocity calibrator. The calibration and linearity were checked before and after each sample run. The linewidth of the inner peaks of natural iron is  $0.26 \text{ mm}/\text{sec}$ .

As the study was devoted to getting a microscopic picture of the type of interaction taking place, measurement of the Curie temperature using the zero-velocity Mössbauer thermal scan method has been used, as this method gives the Curie temperature on a microscopic level. However, this method can only be used when the centroids of the Mössbauer spectra are very close to the zero-velocity channel.<sup>12</sup> In the samples concerned this criterion is fulfilled. Moreover, studies carried out by Burke and Rainford<sup>13</sup> in Fe-Cr alloys have shown that the microscopic and macroscopic measurements of the same quantities gave different results.<sup>14</sup> The zero-velocity scan method has the advantage that it does not require the application of any external magnetic field and, as Mössbauer spectra of some of the samples show coexistence of paramagnetic as well as hyperfine structures, this method is more suitable in the present case. The samples used were identical to the ones prepared for the Mössbauer studies. The samples were then mounted into a vacuum furnace evacuated to  $10^{-5}$  Torr. The temperature was kept fixed within  $\pm 0.5$  to  $\pm 5^\circ\text{C}$  at worst by means of a conventional temperature controller. The counts were collected for 0.5 min at each temperature after allowing for a 5-min stabilization time between each reading (i.e., temperature setting) so as to ensure the establishment of proper temperature equilibrium. Aluminum foils of just enough thickness to cut off the 6-keV x rays were kept between the source and the absorber. Counts were also taken at the beginning and end of each run without any sample but with all other things the same to check for any change in the counting rate. Typical plots of counts versus temperature so obtained for the  $\text{Fe}_3\text{Al}$  samples are shown in Fig. 2. The temperature for

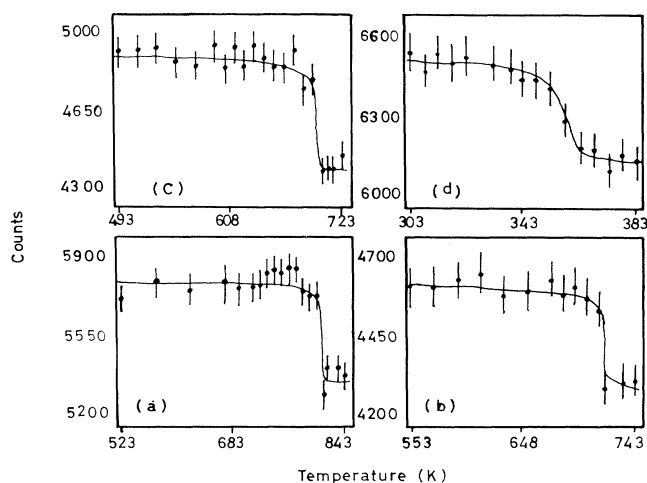


FIG. 2. Zero-velocity Mössbauer thermal scan for (a)  $\text{Fe}_3\text{Al}$  (quenched), (b)  $\text{Fe}_3\text{Al}$  (annealed), (c) and (d)  $\text{Fe}_{3-x}\text{Cr}_x\text{Al}$  alloy,  $x=0.10$  and  $x=0.90$ , respectively.

the sharpest dip in the count rate has been taken as the transition temperature.

### III. RESULTS AND DISCUSSION

#### A. Analysis

The samples of  $\text{Fe}_3\text{Al}$  both quenched and annealed were analyzed using the Meerwal program<sup>15</sup> which fits for sets of Lorentzians. These Lorentzians were fitted for two sets of sextets. The criterion considered for a good fit was a minimum  $\chi^2$  with convergence on increasing the number of iterations. The values of the magnetic hyperfine fields so obtained for the quenched sample were 289 and 259 kOe. The width of the sextets which gave the best fit with this method was found to be 0.79 mm/sec. The values of both fields and widths were found to be unacceptable. In the case of the annealed sample of  $\text{Fe}_3\text{Al}$ , the values of the magnetic hyperfine fields were 288 and 210 kOe. Although the field values are more or less suitable, widths in this case too were too much (0.58 mm/sec). The width of iron peaks is 0.26 mm/sec. The widths of both the  $\text{Fe}_3\text{Al}$  samples fitted by the Meerwal method indicated the presence of a distribution in the hyperfine fields. All the spectra were therefore fitted for a distribution of hyperfine fields using Window's method.<sup>16</sup> This method is ideally suited where the spectra are not well resolved, particularly in the case of the spectra obtained for  $\text{Fe}_{3-x}\text{Cr}_x\text{Al}$ , for  $x$  above 50% where the presence of the paramagnetic part in addition to the hyperfine spectra complicates the spectra.

It had been pointed out by several authors<sup>17-19</sup> that, while using Window's method, it is necessary to determine the proper fitting parameters. The spectra were fitted with the constraint that linewidth  $\Gamma$  be that corresponding to  $\alpha\text{-Fe}$ . [It was seen that  $\chi^2$  was minimal for  $\Gamma = \Gamma(\alpha\text{-Fe})$ . Width of  $\alpha\text{-Fe}$  was seen to be 0.26 mm/sec]. The number of cosine terms found to be most suitable was 8. Negative oscillations in the  $P(H)$  distribution do not have any physical meaning.

#### B. $\text{Fe}_3\text{Al}$ (quenched)

The Mössbauer spectra of the quenched  $\text{Fe}_3\text{Al}$  sample at room temperature and the hyperfine-field distribution obtained are shown in Fig. 3. It has been pointed out by Fultz, Gao, and Hamdeh<sup>20</sup> that heating  $\text{Fe}_3\text{Al}$  at 800°C leads to the loss of both  $D0_3$  as well as  $B2$  long-range ordering. The spectrum reported by them for their quenched sample compares rather well with that of our own quenched sample. The hyperfine-field distribution for this sample of  $\text{Fe}_3\text{Al}$  is broad and shows the presence of two major components [Fig. 3(b)]. One is a high-field component (hereafter called  $H_2$ ) appearing around 265 kOe and the other a low-field one (hereafter called  $H_1$ ) at 155 kOe. Of the two,  $H_2$ , i.e., corresponding to 265 kOe, is more intense and has a width of 80 kOe while  $H_1$  (at 155 kOe) has a width of 45 kOe. The fractional widths of both components  $\Delta H/H$ , therefore work out to be 0.3. The average hyperfine field obtained from the hyperfine-field distribution analysis of the Mössbauer spectrum is a

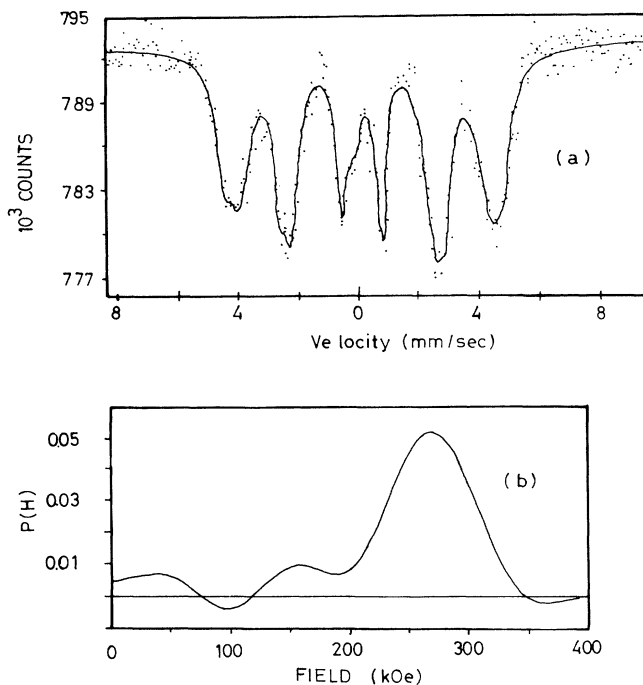


FIG. 3. Mössbauer spectrum (a) and hyperfine-field distribution (b) of  $\text{Fe}_3\text{Al}$  (quenched) alloy at room temperature.

weighted average of the individual components and is 239 kOe for the sample. This value is comparable with the value reported by Frackowiak<sup>21</sup> for disordered  $\text{Fe}_3\text{Al}$  prepared by quenching from 950°C into ice brine. As pointed out earlier, the manner of heat treatment imparted to  $\text{Fe}_3\text{Al}$  plays a very strong role in determining the final parameters shown by this alloy. The values of the average hyperfine field ( $H_{av}$ ), widths of the components,  $\Delta H_1$  and  $\Delta H_2$ , as well as  $\Delta H/H$  for both the field components are shown in Table I.

The Curie temperature of this sample (measured by zero-velocity Mössbauer thermal scan method) is 810 K and matches well with that reported for disordered  $\text{Fe}_3\text{Al}$  by Tuszynski, Zarek, and Popiel.<sup>22</sup> A comparison of the field distribution obtained for this sample with that obtained by Fultz, Gao, and Hamdeh<sup>20</sup> allows the assignment of the number of nearest-neighbor Al atoms associated with these sites. Accordingly, the high-field component of 265 kOe can be attributed to a configuration 2–3 nearest-neighbor Al and that at 155 kOe having 5 nearest-neighbor Al, respectively.

The broad peaks present in the hyperfine distribution of this sample can be understood as arising from the disorder present in this material. The first systematic investigation for Fe-Al alloys in the range 20–30 at. % Al was made by Bradley and Jay.<sup>23</sup> They found that alloys containing more than 20 at. % Al form configurations based on both the  $B2$  as well as  $D0_3$  type superlattices. The  $B2$  structure is of the CsCl type, i.e., in which there is a complete disorder between the atoms on the  $[B]$  and  $[D]$  sites. While this does represent considerable disorder as compared to the  $D0_3$  type of structure, a good deal of long-

TABLE I. Internal magnetic fields, fractional width of the fields, and Curie temperatures for Fe<sub>3</sub>Al. The internal field components  $H_1$  and  $H_2$  were determined from the subpeaks in the hyperfine-field distributions.

Sample	$H_{av}$ (kOe)	$H_1$ (kOe)	$H_2$ (kOe)	$\Delta H_1/H_1$	$\Delta H_2/H_2$	$T_C$ (K)
Fe <sub>3</sub> Al (quenched)	239.1 240.0 <sup>a</sup>	155	265	0.29	0.30	810 810 <sup>b</sup>
Fe <sub>3</sub> Al (annealed)	223.3	215 211±3.3 <sup>c</sup>	290 293.7±3.3 <sup>c</sup>	0.20	0.14	720 713 <sup>c</sup>

<sup>a</sup>Value for disordered alloy taken from Fig. 1(b) of Ref. 21.

<sup>b</sup>Value for disordered alloy taken from Fig. 1(a) of Ref. 22.

<sup>c</sup>Reported values for ordered alloy taken from Ref. 5.

range order still exists. According to Taylor and Jones,<sup>24</sup> B2-type pseudo-order begins to form at Al concentrations below 25 at. % and the ordering occurs very rapidly. The studies of Fe-Al system by Pál and Tornoczi<sup>25</sup> with 23–25 % Al show that a completely ordered phase which is also ferromagnetic can be formed at 490 °C. As in the formation of our sample, the sample was never held at temperatures conducive to ordering and was quenched from 800 °C, disorder is frozen at room temperature.

The value of  $\Delta H/H$  being equal to 0.3 in both high- and low-field component sites in the disordered Fe<sub>3</sub>Al sample shows that the distribution in the number of Al atoms around both these sites about the most probable values of 5 and 2–3 are the same for both sites. This implies that with the increase in the disorder, the probability of an iron atom seeing more and more Al as nearest neighbors increases leading to a shift in the corresponding field components in the probability distribution curves. In the fully ordered state, the two Fe sites have four and zero nearest-neighbor Al, respectively. Correspondingly, the value of fields at these sites is higher than those seen in disordered Fe<sub>3</sub>Al.

From the study of Fe<sub>3</sub>Al in disordered states we conclude that heating at 800 °C and then quenching the sample holds the sample at almost a state of complete chemical disorder. Order is present only in the short-range limit. Moreover, two most probable configurations for Fe atoms exist in highly disordered Fe<sub>3</sub>Al which are one with 5 nearest-neighbor Al and the other with 2–3 nearest-neighbor Al. The amount of disorder existing in these sites individually is about 30% each.

### C. Fe<sub>3</sub>Al (annealed)

This sample was prepared by allowing Fe<sub>3</sub>Al to cool down to room temperature from the annealing temperature of 800 °C at the rate of 50 °C/h. The presence of two sextets was visible in the spectrum indicating the evolution of better ordering. The figures of the Mössbauer spectrum as well as the hyperfine distribution obtained for the sample are shown in Fig. 4. It can be seen that the broad distribution narrowed considerably ( $\Delta H_1/H_1=0.2$ ,  $\Delta H_2/H_2=0.14$ ) and showed two components of almost equal intensity. The intensity which is measured by the height of the distribution peaks indicates

the probability of the probe Fe (which is also a constituent here) to find itself in the presence of corresponding hyperfine fields. Equal intensities, therefore, indicate the equal probability for the Fe to find itself at fields which are 285 and 210 kOe, respectively, in this sample. The values of hyperfine field observed in our sample are close to those reported by Grandjean and Gerard<sup>26</sup> and Stearns.<sup>27</sup> The small difference in the values of hyperfine fields in our sample compared to earlier studies can be attributed to the fact that the observed values are strongly dependent on the temperature treatment.

The decrease in the value of the higher-field component from 285 kOe (in the annealed sample) to 265 kOe (in the quenched one) over a change in the ordering, i.e., from a fully ordered to nearly fully disordered state can be understood in terms of the number of nearest-neighbor Al atoms seen by Fe in Fe<sub>3</sub>Al. The hyperfine fields in

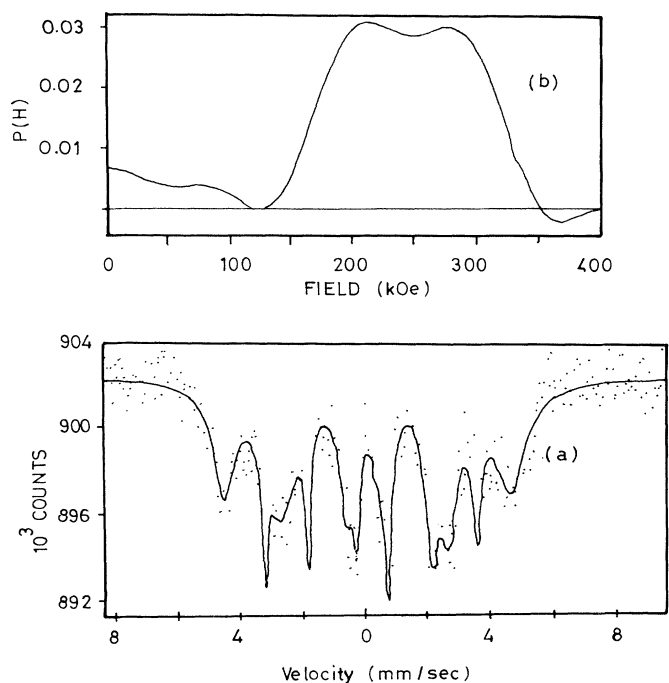


FIG. 4. Mössbauer spectrum (a) and hyperfine-field distribution (b) of Fe<sub>3</sub>Al (annealed) alloy at room temperature.

$\text{Fe}_3\text{Al}$  alloys are particularly sensitive to the nearest-neighbor configurations. Neutron-diffraction studies of ordered  $\text{Fe}_3\text{Al}$  show that magnetic moments at Fe at the two sublattices, i.e., Fe[A,C] and Fe[B] are substantially different. Their values were worked out to be  $1.46 \pm 0.1\mu_B$  at Fe[A,C] and  $2.14 \pm 0.1\mu_B$  at Fe[B] sites, respectively, by Stearns<sup>27</sup> as well as Ono, Ishikawa, and Ito.<sup>28</sup> Both have carried Mössbauer studies on well-ordered  $\text{Fe}_3\text{Al}$ . In the  $\text{DO}_3$  type of structure which is the configuration for the perfectly long-range-ordered form of this alloy, the iron atom at B site, i.e., Fe[B] has eight Fe atoms as nearest neighbors, i.e., the iron at this site has no Al atoms at the nearest-neighbor site. The environment that Fe[B], therefore, finds itself in is nearly identical to that of Fe in pure iron. So the field observed at this site will be close to the 330 kOe observed in pure iron (in fact, in the fully ordered state it is about 300 kOe). The field is still not equal to that of pure iron because of the presence of Al as second-nearest neighbors, which reduces the overall field at the Fe[B] site. The lower-field component is associated with the Fe in the [A,C] site. Fe[A,C] has four Fe and four Al as first-

nearest neighbors and the 3d shells of the [A,C]-type iron atoms are preferably occupied by electrons from the less electronegative aluminum atoms. The aluminum atoms themselves do not carry any magnetic moments. This leads to a state where there are not enough electrons with uncompensated spins leading to a magnetic interaction. The effect is that the magnetic moment of Fe[A,C] is decreased, leading to a decrease in the hyperfine field at this site as compared to that present in pure Fe.

#### D. $\text{Fe}_{3-x}\text{Cr}_x\text{Al}$ alloys

The Mössbauer spectra and the hyperfine-field distribution for the series  $\text{Fe}_{3-x}\text{Cr}_x\text{Al}$  for  $x$  ranging from 0 to 1.0 taken at room temperature are shown in Figs. 5 and 6, respectively. As can be observed from the Mössbauer spectra with increase in the concentration of chromium, the overall spread in the Mössbauer envelope becomes smaller, indicating an overall decrease in the magnetic hyperfine field. The 50% Cr sample shows the beginning of the development of a zero hyperfine, i.e., a paramagnetic peak along with the hyperfine structure. The spectrum for the composition  $\text{Fe}_2\text{CrAl}$ , i.e.,  $x=1.0$ , shows mainly a paramagnetic peak with very small hyperfine

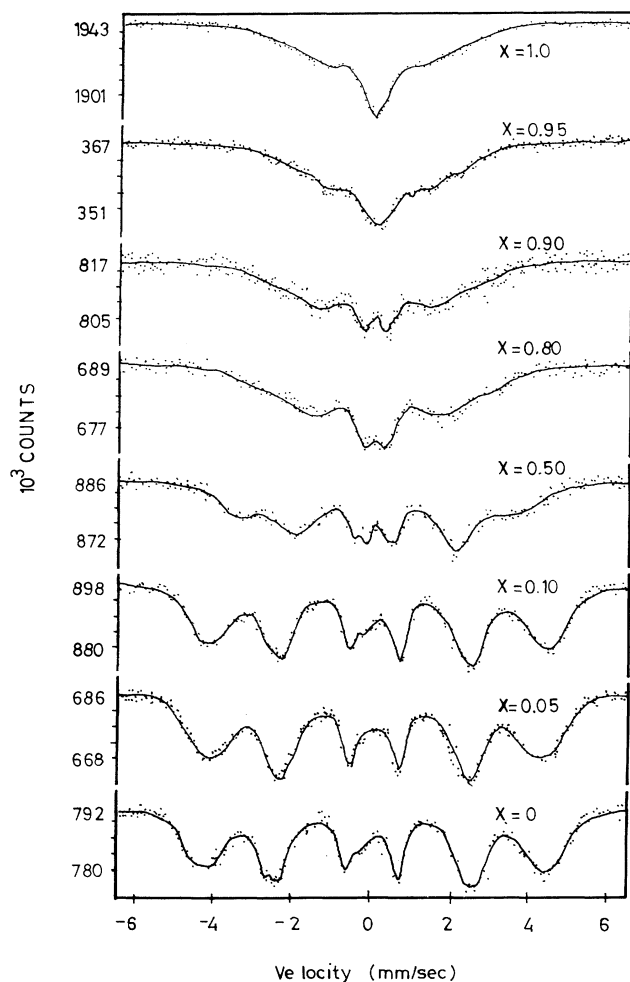


FIG. 5. Mössbauer spectra of  $\text{Fe}_{3-x}\text{Cr}_x\text{Al}$  alloys at room temperature.

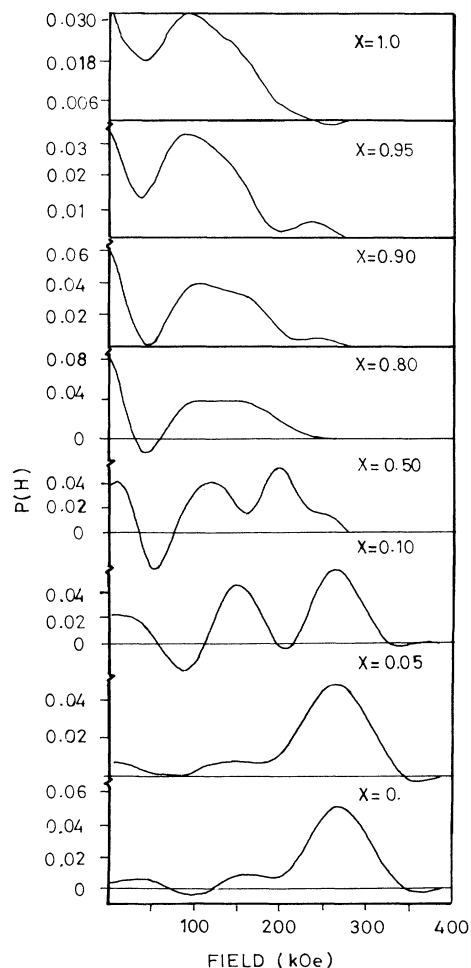


FIG. 6. Hyperfine-field distributions of  $\text{Fe}_{3-x}\text{Cr}_x\text{Al}$  alloys.

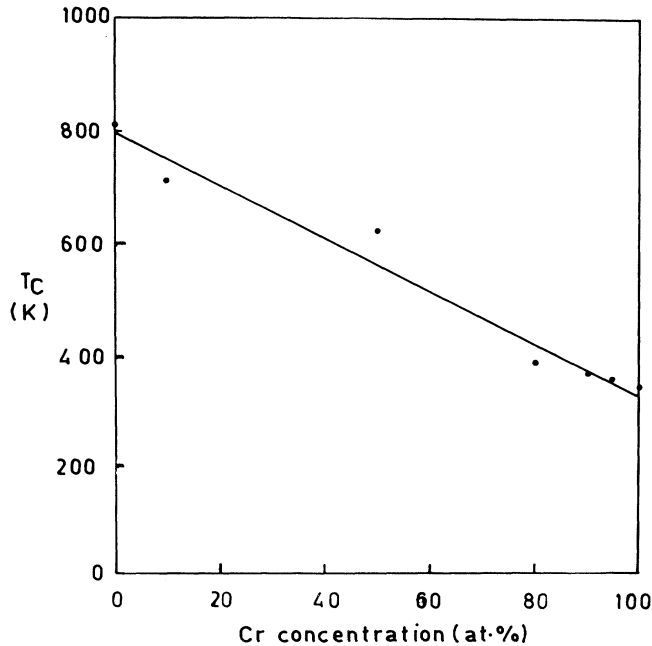


FIG. 7. Variation of Curie temperature with chromium concentration for  $\text{Fe}_{3-x}\text{Cr}_x\text{Al}$  alloys.

fields. The variation of Curie temperature with chromium concentration is linear and is shown in Fig. 7.

The Mössbauer spectra have been recorded at room temperature which for all the samples lies well below their Curie temperatures. Fitting for the experimental data was done by Window's<sup>16</sup> method of fitting for a distribution in the hyperfine fields.

The Mössbauer spectra show that these materials have formed disordered systems. However, the substitution of iron by chromium shows some interesting results.

On examining the  $P(H)$  curves plotted for each of these spectra, keeping the parameters the same as in the fitting procedure described earlier, it can be seen that the high-field peak steadily decreases in intensity and also goes on shifting to lower values of field (Table II). The lower peak instead grows in such a way that the change

TABLE II. Internal magnetic fields, fractional width of the fields, and Curie temperatures for the  $\text{Fe}_{3-x}\text{Cr}_x\text{Al}$  system for  $x=0-1.0$ .

Cr content (at. %)	$H_{av}$ (kOe)	$H_1$ (kOe)	$H_2$ (kOe)	$\Delta H_1/H_1$	$\Delta H_2/H_2$	$T_C$ (K)
0	239.1	155	265	0.29	0.30	810
5	235.8	140	265	0.45	0.34	760
10	233.0	150	265	0.33	0.24	710
50	194.1	135	215	0.48	0.26	620
80	144.0	120	170	0.58	0.50	390
90	138.0	120	160	0.33	0.56	370
95	101.0	110	145	0.82	0.55	350
100	80.0	90	145	1.00	0.43	348

with ratio of intensities (height of peak in the probability distribution) of the lower-field peak  $H_1$  to that of the higher-field one  $H_2$ , with the concentration of Cr goes on increasing as shown in Fig. 8(a).

Figure 8(b) shows the change in the values of each of the two components with increasing concentration of Cr. The change shown by both fields is linear with concentration of Cr. As can be seen, over the range considered, the value of the lower field remains almost constant as compared to the change of the higher-field peak. The total shift, i.e., the change in the hyperfine field over the entire concentration range of 0–100% in chromium, is only 65 kOe. The shift in the higher peak is faster with the change in field from 0 to 100% in Cr seen to be 120 kOe. This implies a slope twice as steep as that for  $H_1$ . The average hyperfine-field (Fig. 9) variation with concentration of Cr is seen to be nonlinear because of the appearance of the paramagnetic portion in the distribution. The spread in the field distribution is in general seen to increase with concentration.

As pointed out earlier, in  $\text{Fe}_3\text{Al}$ , the hyperfine field at iron is very sensitive to local or neighboring environment. Naturally, as compared to a completely ordered system, where 1 iron, Fe[B], is surrounded by 8 iron and the other, Fe[A, C], by 4 each of iron, i.e., in terms of Al corresponding to 0 nearest neighbor and 4 nearest neighbor,

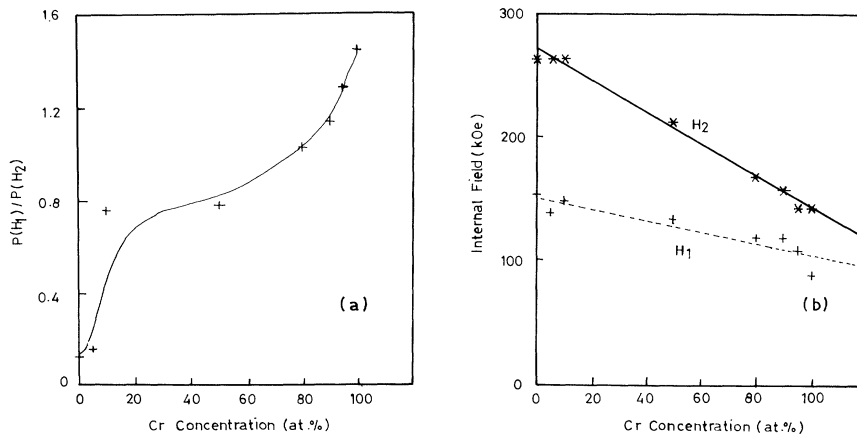


FIG. 8. Variation of (a) ratio of probabilities of hyperfine-field components and (b) hyperfine-field components with chromium concentration for  $\text{Fe}_{3-x}\text{Cr}_x\text{Al}$  alloys.

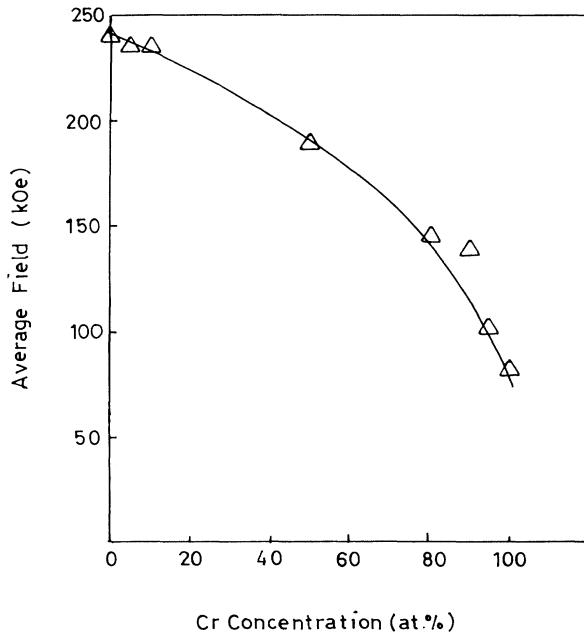


FIG. 9. Variation of average hyperfine field with chromium concentration for  $\text{Fe}_{3-x}\text{Cr}_x\text{Al}$  alloys.

the higher peak corresponds to what would have been the  $\text{Fe}[B]$  site, in the fully ordered structure, and the lower one the  $\text{Fe}[A, C]$  site. The peak in the hyperfine-field distribution at  $H_2$  in  $\text{Fe}_{3-x}\text{Cr}_x\text{Al}$  is shifted to the left, i.e., towards lower field compared to ordered  $\text{Fe}_3\text{Al}$ . This site in  $\text{Fe}_3\text{Al}$  can be associated with 2–3 nearest-neighbor Al as seen in the preceding section. Since the heat treatment has remained the same and replacement of only Fe and not Al has been effected, this field can still be associated as having 2–3 nearest-neighbor Al. In simple terms, the magnetic moment being felt by iron in this site has been diluted by the presence of Al atoms as nearest neighbors, as Al being nonmagnetic does not contribute to the magnetic field. But as seen, there is a systematic decrease in this (higher) hyperfine field with the increase in the Cr content. In addition, the ratio of intensities of the probability distributions between the lower field and the higher one shows a steady and nearly linear increase tending to level off at a concentration of 90%. This clearly shows that although the alloys are disordered, there is a clear site preference for the substituted chromium. The chromium mostly goes into that site which has fewer Al as nearest neighbors. This accounts for the steep decrease in the magnetic field in the iron which has the higher magnetic moment and the very small slope of the field versus concentration curve of the lower-field Fe. The appearance of a paramagnetic part coexisting with the hyperfine distribution has been observed in Fe-Cr alloys which, like the present samples, are chemically homogeneous. This has also been observed in  $\text{Fe}_{3-x}\text{V}_x\text{Al}$  alloys and can be explained as arising due to the presence of clusters. Clusters screen the Fe atom from the neighboring influences and so those Fe atoms

which have clusters do not feel the magnetic hyperfine field giving rise to a paramagnetic peak in the spectrum.

A change in the hyperfine field means a change in the spin density. Many authors,<sup>29–33</sup> in trying to explain the value of the hyperfine field at Fe nuclei in metallic iron, give a relation between the change of the field and the corresponding change of the number of polarized electrons.<sup>29</sup> As there exist a lot of discrepancies in these reported values of the actual estimation in the number of electrons to effect a change in the field, no attempt has been made to calculate the number.

Tuszynski, Zarek, and Popiel<sup>22</sup> studied the magnetic properties of chemically disordered  $\text{Fe}_{3-x}\text{V}_x\text{Al}$  alloys. They found that the variation of the Curie temperature with concentration was nearly linear. It was also seen that the variation of the average magnetic moment also followed the same pattern. From this they concluded that the V atoms do not have local magnetic moment. The Mössbauer spectra showed the coexistence of a single line with the hyperfine structure which led to the conclusion that an increase in the substitution of Fe by V led to magnetic disordering borne out by a broadening in the hyperfine distribution as well as a shift towards lower fields. Despite the chemical homogeneity, the authors concluded that magnetic clusters were present in this system even in fully ordered alloys as indicated by the Mössbauer spectra showing the coexistence of paramagnetic as well as hyperfine structures (i.e., magnetically disordered despite being chemically ordered). The system  $\text{Fe}_{3-x}\text{Cr}_x\text{Al}$  also showed similar behavior with the increase in the substitution of Fe by Cr atoms. However, Cr couples antiferromagnetically with Fe or in general the direction of magnetization of the alloy, Fe being the only magnetic atom present, whereas V enters strictly as another nonmagnetic atom. This along with the clustering (of most probably Cr atoms) accounts for the non-linearity seen in the average hyperfine field of this series of alloys.

Substitution of Fe in  $\text{Fe}_3\text{Si}$  with transition metals has been studied in detail by Niculescu *et al.*<sup>34</sup> and Stearns.<sup>27</sup>  $\text{Fe}_3\text{Si}$  is isostructural to  $\text{Fe}_3\text{Al}$  and allows the systematic substitution of various elements. An outcome of these studies is the systematic site preference on substitution with transition elements as already mentioned. Just as in the case of Cr substitution or substituting with Mn, changes in the hyperfine field were observed which were accounted for by taking into consideration the fact that Mn couples antiferromagnetically with Fe or the general direction of alloy magnetization. V substitution, on the other hand, did not show any such effect. Their attempt to make  $\text{Fe}_{3-x}\text{Cr}_x\text{Si}$  series was hampered because of the fact that some of the samples tended to be off-stoichiometric and no NMR signal for Cr was observed. The observed change in the hyperfine fields was explained in terms of change in the conduction-electron polarization terms, i.e., again in terms of the change in the number of polarized 4s-like electrons.

In conclusion, we see that it is possible to induce  $\text{Fe}_3\text{Al}$  at nearly disordered state by quenching the sample from 800 °C. On systematically substituting iron by chromium in  $\text{Fe}_3\text{Al}$  stoichiometrically, to form a series such as

Fe<sub>3-x</sub>Cr<sub>x</sub>Al, it is observed that even though these alloys are disordered, some sort of short-range ordering exists. Though being disordered, the substituted Cr has an almost definite site preference to replace Fe atoms at [A, C] sites. Magnetic disordering increases with increasing Cr concentration through the formation of clusters.

#### ACKNOWLEDGMENTS

We wish to thank Dr. Poulouse, TIFR, Bombay, for providing the hyperfine-field distribution computer program. One of us (N.L.) gratefully acknowledges partial support by CSIR. This work was supported by the UGC DRS program.

- 
- <sup>1</sup>A. R. Miodwrich, *Bull. Alloy Phase Diagr.* **2**, 406 (1982).  
<sup>2</sup>G. Inden, in *Alloy Phase Diagrams*, edited by L. H. Bennett, T. B. Massalski, and B. C. Giessen, MRS Symposia Proceedings No. 19 (Materials Research Society, Pittsburgh, 1983), p. 175.  
<sup>3</sup>G. Inden, *Bull. Alloy Phase Diagr.* **24**, 412 (1982).  
<sup>4</sup>M. C. Cadeville and J. L. Moran-Lopez, *Phys. Rep.* **153**, 331 (1987).  
<sup>5</sup>M. B. Stearns, *Phys. Rev.* **168**, 588 (1968).  
<sup>6</sup>S. M. Dubiel, Ch. Sauer, and W. Zinn, *Phys. Rev. B* **32**, 2745 (1988).  
<sup>7</sup>W. A. Hines, A. H. Menotti, J. I. Budnick, T. Litrenta, V. Niculescu, and K. Raj, *Phys. Rev. B* **13**, 4060 (1976).  
<sup>8</sup>V. Niculescu, K. Raj, J. I. Budnick, T. J. Burch, W. A. Hines, and A. H. Menotti, *Phys. Rev. B* **14**, 4160 (1976).  
<sup>9</sup>T. Kamimori, *J. Sci Hiroshima Univ. Ser. A: Phys. Chem.* **51**, 41 (1987).  
<sup>10</sup>N. K. Jaggi, K. R. P. M. Rao, A. K. Grover, L. C. Gupta, R. Vijayaraghavan, and Le Dang Khoi, *Hyperfine Interact.* **4**, 402 (1978).  
<sup>11</sup>G. K. Wertheim and J. H. Wervick, *Acta Metall.* **15**, 297 (1967).  
<sup>12</sup>R. W. Grant, in *Mössbauer Spectroscopy*, edited by U. Gonser, Topics in Applied Physics Vol. 5 (Springer-Verlag, Berlin, 1975).  
<sup>13</sup>S. K. Burke and B. D. Rainford, *J. Phys. F* **13**, 471 (1983).  
<sup>14</sup>B. Loegel, *J. Phys. F* **5**, 497 (1975).  
<sup>15</sup>E. V. Meerwal, *Comput. Phys. Commun.* **9**, 117 (1975).  
<sup>16</sup>B. Window, *J. Phys. E* **4**, 401 (1971).  
<sup>17</sup>G. H. Whittle, S. J. Campbell, and A. M. Stewart, *Phys. Status Solidi A* **71**, 245 (1982).  
<sup>18</sup>R. A. Dunlap and G. Stroink, *Can. J. Phys.* **62**, 714 (1984).  
<sup>19</sup>H. Keller, *J. Appl. Phys.* **52**, 5268 (1981).  
<sup>20</sup>B. Fultz, Zheng-Qiang Gao, and H. Hamdeh, *Hyperfine Interact.* **54**, 521 (1990).  
<sup>21</sup>J. E. Frackowiak, *Hyperfine Interact.* **54**, 793 (1990).  
<sup>22</sup>M. Tuszynski, W. Zarek, and E. S. Popiel, *Hyperfine Interact.* **59**, 369 (1990).  
<sup>23</sup>A. I. Bradley and A. H. Jay, *Proc. R. Soc. London Ser. A* **136**, 210 (1932).  
<sup>24</sup>A. Taylor and R. M. Jones, *J. Phys. Chem. Solids* **6**, 16 (1958).  
<sup>25</sup>L. Pál and Tornoczi, *J. Phys. Chem. Solids* **23**, 683 (1962).  
<sup>26</sup>F. Grandjean and A. Gerard, *J. Magn. Magn. Mater.* **1**, 64 (1975).  
<sup>27</sup>M. B. Stearns, *Phys. Rev. B* **17**, 2809 (1971).  
<sup>28</sup>K. Ono, Y. Ishikawa, and A. Ito, *J. Phys. Soc. Jpn.* **17**, 1747 (1962).  
<sup>29</sup>S. M. Dubiel, *Hyperfine Interact.* **8**, 291 (1980).  
<sup>30</sup>S. Wakoh and J. Yamashita, *J. Phys. Soc. Jpn.* **21**, 1712 (1966); **25**, 1272 (1968).  
<sup>31</sup>R. E. Watson and A. J. Freeman, *Phys. Rev.* **123**, 2027 (1961).  
<sup>32</sup>D. A. Goodings and V. Heine, *Phys. Rev. Lett.* **5**, 370 (1960).  
<sup>33</sup>K. J. Duff and T. P. Das, *Phys. Rev. B* **3**, 2294 (1971).  
<sup>34</sup>V. Niculescu, K. Raj, T. J. Burch, and J. I. Budnick, *Phys. Rev. B* **13**, 3167 (1976).